Appendix: Characterization of Normal and Malignant Breast Tissues utilizing Hyperspectral Images and Associated Differential Spectrum Algorithm

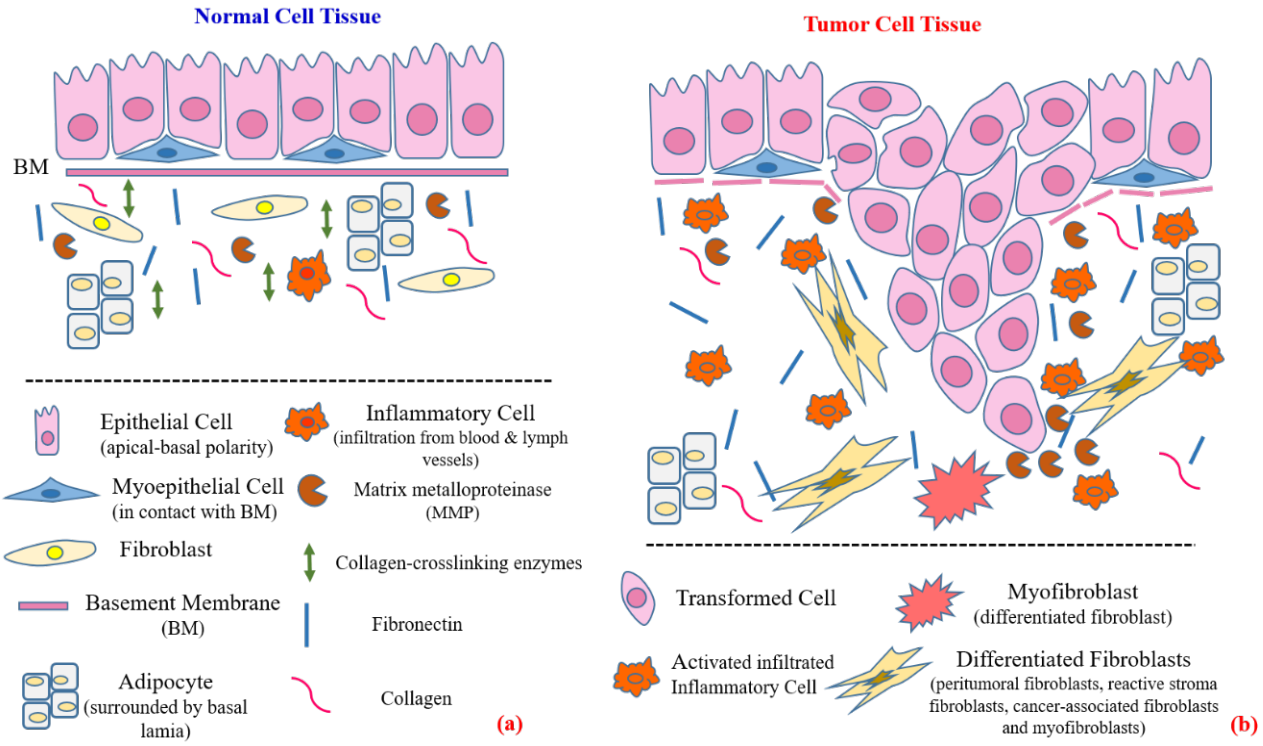

Fig. A1 The function and the structure of the extracellular matrix to highlight the effect of changing tissues in changing the movement of light and its reflections; (a) normal breast cell tissue; (b) tumor breast cell tissue.

Table A1 The patient data for the investigated samples exploited in the presented study.

No	Patient ID	Age (years)	Breast Density	Breast Cancer Type	Pathological Report	Tumor Phase	Score
	Patient#1001	49	Type D	Invasive Ductal Carcinoma (IDC)	Malignant	Phase I (≥4cm in diameter)	Score III
	Patient#1002	53	Type C	Invasive Ductal Carcinoma (IDC)	Malignant	Phase III (>4cm in diameter but confined to the breast)	Score II
	Patient#1003	49	Type D	Invasive Ductal Carcinoma (IDC)	Malignant	Phase II (<4cm in diameter)	Score I
	Patient#1004	54	Type B	Invasive Ductal Carcinoma (IDC)	Malignant	Phase II (<4cm in diameter)	Score II
	Patient#1005	60	Type C	Invasive Ductal Carcinoma (IDC)	Malignant	Phase II (<4cm in diameter)	Score I
	Patient#1006	65	Type D	Invasive Ductal Carcinoma (IDC)	Malignant	Phase II (<4cm in diameter)	Score II
	Patient#1007	46	Type D	Invasive Ductal Carcinoma (IDC)	Malignant	Phase III (>4cm in diameter but confined to the breast)	Score I
	Patient#1008	58	Type D	Invasive Ductal Carcinoma (IDC)	Malignant	Phase II (<3cm in diameter)	Score II
	Patient#1009	50	Type B	Invasive Ductal Carcinoma (IDC)	Malignant	Phase I (<2cm in diameter)	Score I
	Patient#1010	56	Type C	Invasive Ductal Carcinoma (IDC)	Malignant	Phase III (>3cm in diameter but confined to the breast)	Score II

Tumor Score:
Score I – Well differentiated.
Score II – Moderately differentiated.

Tumor Phase:
Phase I – The Breast Cancer is ≤ 2 cm diameter and the Tumor has not spread beyond the breast.
Phase II – The Breast Cancer is 2 ~4 cm diameter or malignant cells have spread to the lymph nodes in the underarm area.
Phase III – The Breast Cancer is widespread identified; however, it is confined to the breast, surrounding tissues.

Breast Density with respect to the "American College of Radiology (ACR):
Type A Fatty Breast.
Type B Scattered Density Breast.
Type C Heterogeneously Density Breast.
Type D Extremely Density Breast.

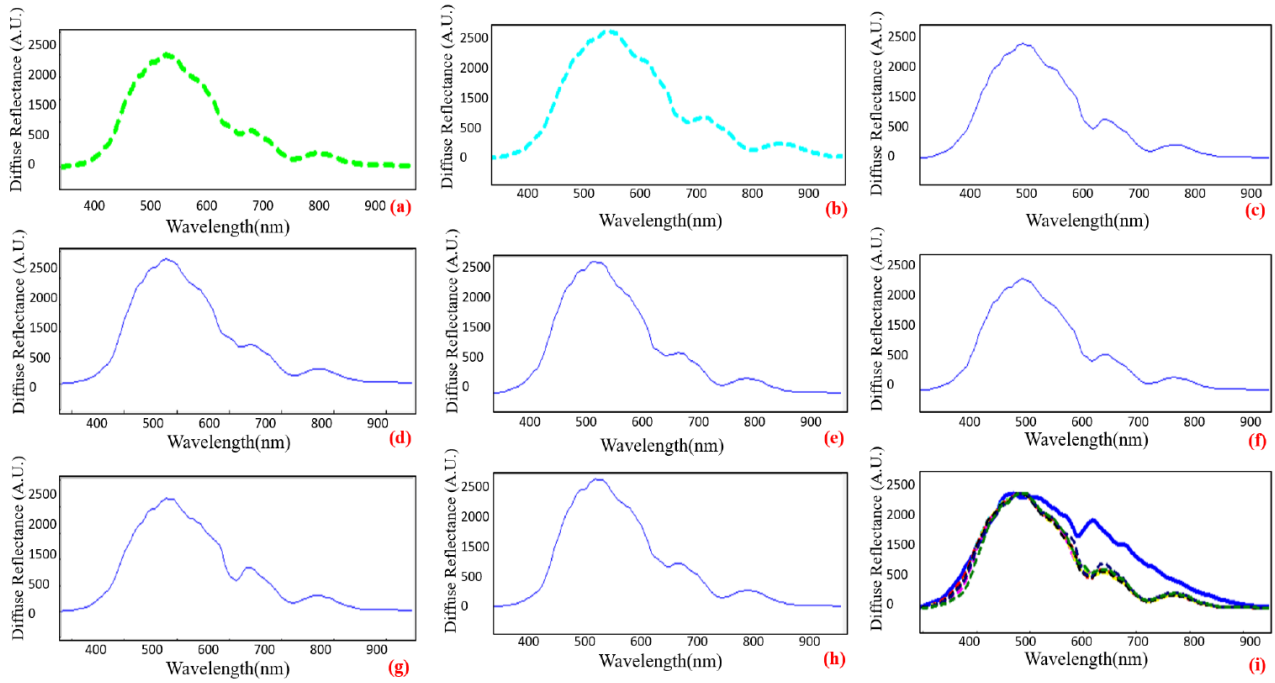

Fig. A2 The Worksheet for the Measured Diffuse Reflection (R_d) of the normal tissue for Different Eight-investigated *ex vivo* breast samples highlighting the system reliability; (a) The measured (R_d) for the normal tissue of Sample #1 , (b) The measured (R_d) for the normal tissue of Sample #2, (c) The measured (R_d) for the normal tissue of Sample #3, (d) The measured (R_d) for the normal tissue of Sample #4, (e) The measured (R_d) for the normal tissue of Sample #5, (f) The measured (R_d) for the normal tissue of Sample #6, (g) The measured (R_d) for the normal tissue of Sample #7, (h) The measured (R_d) for the normal tissue of Sample #8, (i) The combination of the whole signals hilighting the measured (R_d) for the normal tissue of the investigated eight-samples regards the source light reference.

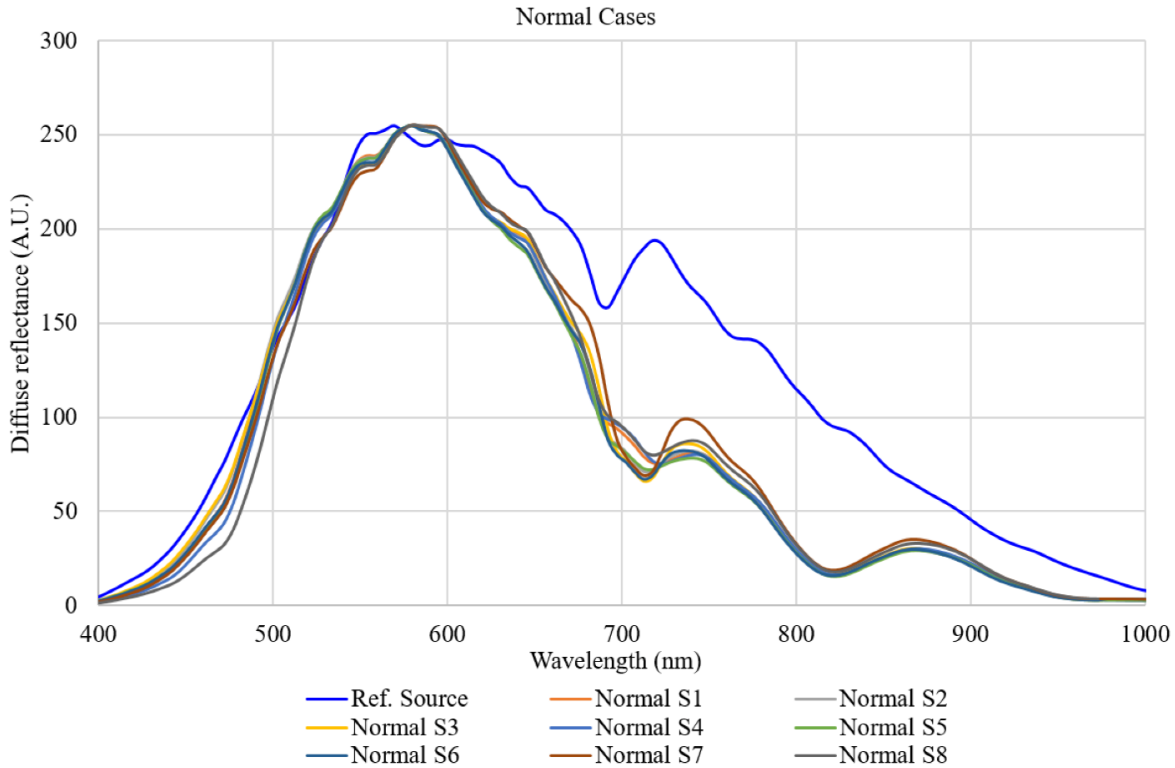

Fig. A2 (i) The magnified image for the combination diffuse reflection (R_d) signals of the normal tissue for the investigated eight-samples regards the source light reference.

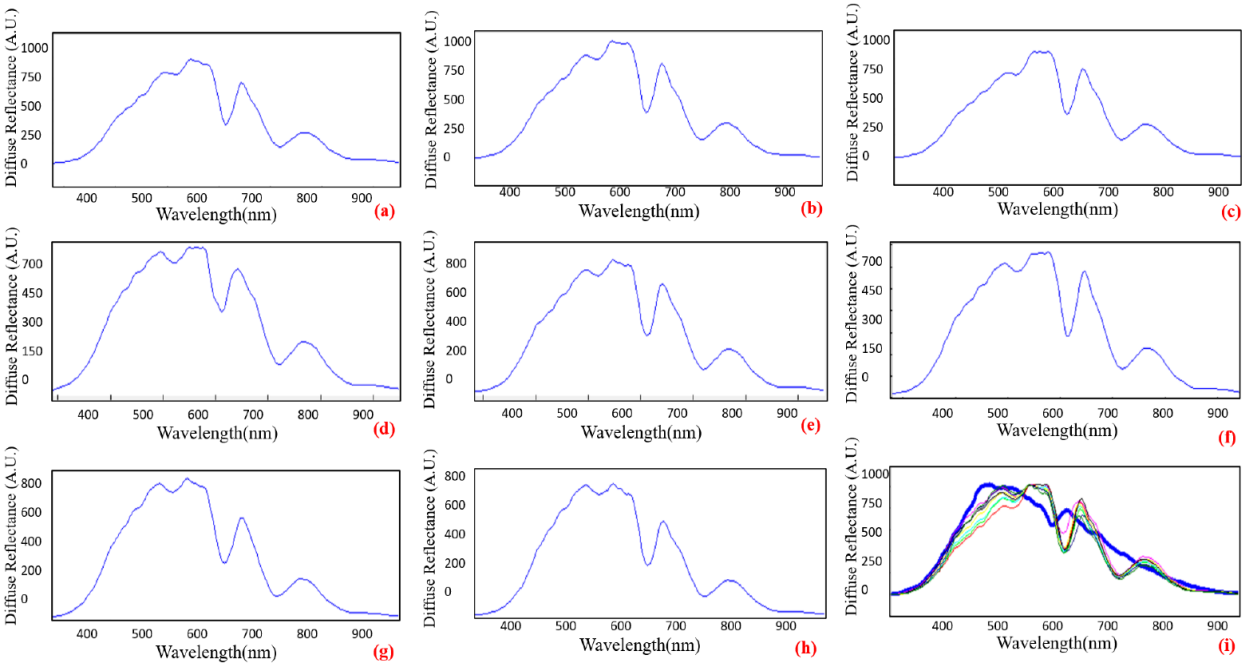

Fig. A3 The worksheet for the measured diffuse reflection (R_d) of the tumor tissue for different eight-investigated *ex vivo* breast samples highlighting the system reliability; (a) the measured (R_d) for the tumor tissue of Sample #1, (b) the measured (R_d) for the tumor tissue of Sample #2, (c) the measured (R_d) for the tumor tissue of Sample #3, (d) the measured (R_d) for the tumor tissue of Sample #4, (e) the measured (R_d) for the tumor tissue of Sample #5, (f) the measured (R_d) for the tumor tissue of Sample #6, (g) the measured (R_d) for the tumor tissue of Sample #7, (h) the measured (R_d) for the tumor tissue of Sample #8, (i) the combination of the whole signals hilighting the measured (R_d) for the tumor tissue of the investigated eight-samples regards the source light reference.

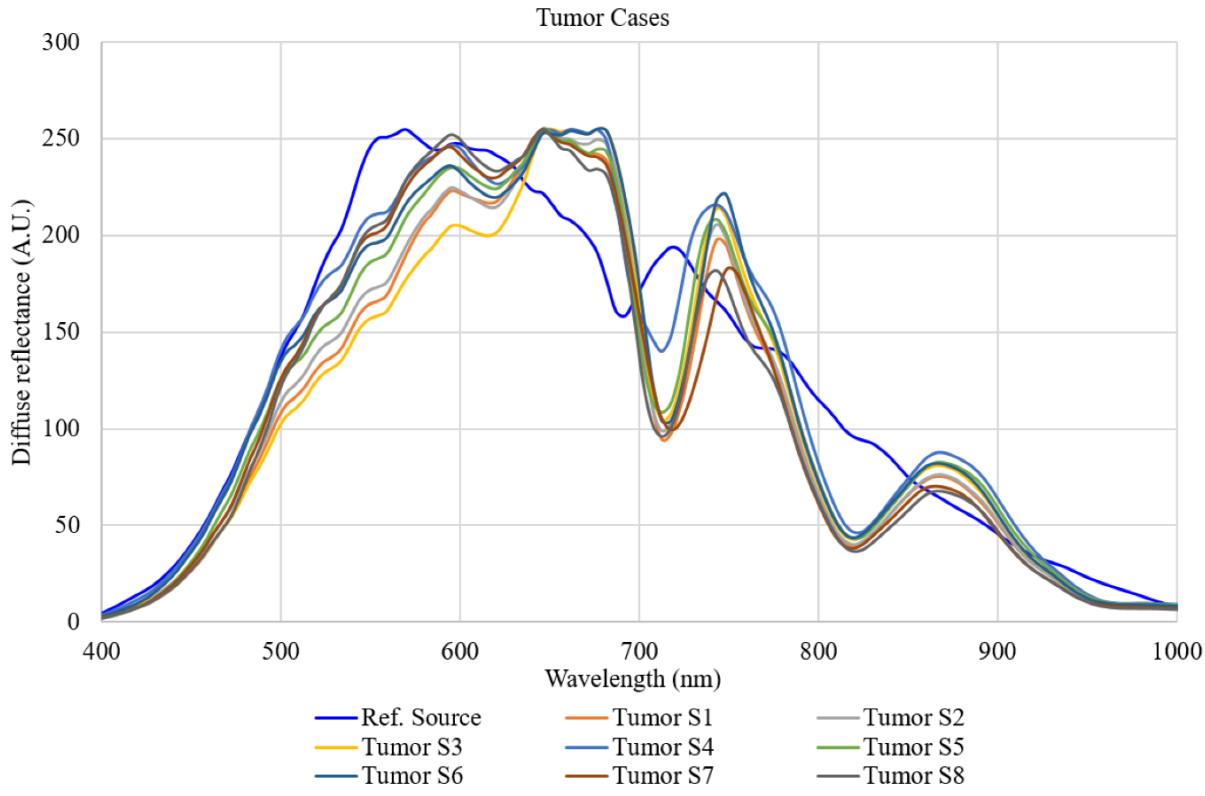

Fig. A3 (i) The magnified image for the combination diffuse reflection (R_d) signals of the tumor tissue for the investigated eight-samples regards the source light reference.

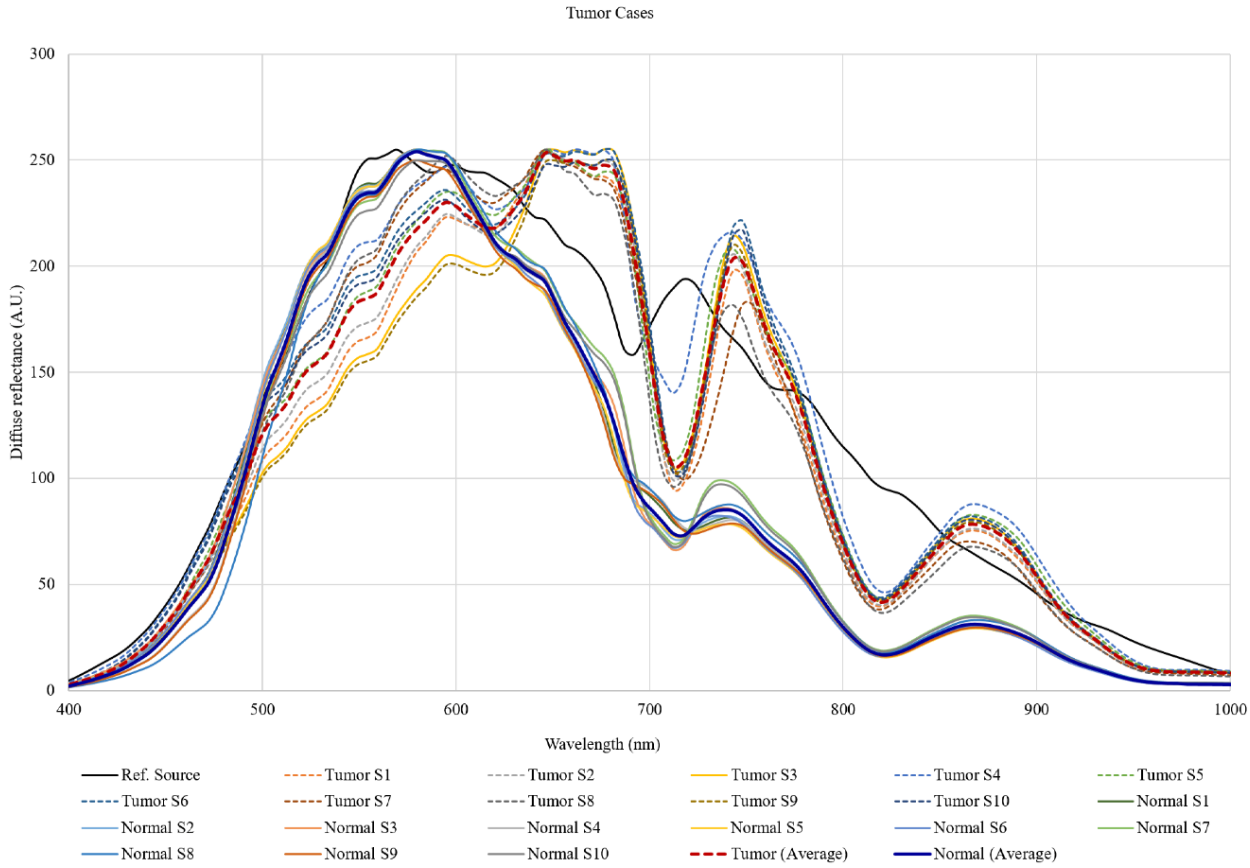

Fig. A4 The combination of the measured diffuse reflection (Rd) signals for the investigated normal tissue regions and the tumor regions of the ten ex-vivo breast samples with respect to the source light reference.

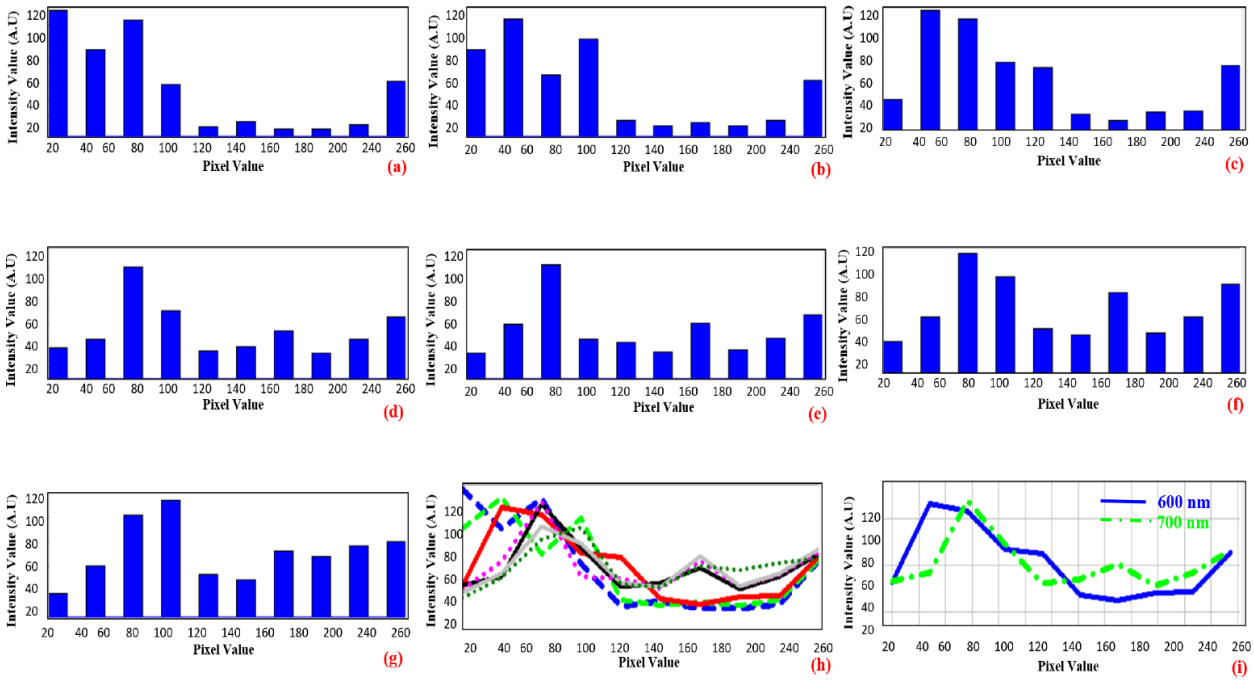

Fig. A5 The histogram of the selected spectral images, (a) spectral image of the investigated sample at wavelength 400 nm, (b) wavelength 500 nm, (c) wavelength 600 nm, (d) wavelength 700 nm, (e) wavelength 800 nm, (f) wavelength 900 nm, (g) wavelength 1000 nm, (h) the histogram analysis of the seven spectral images (400–1000 nm), (i) the histogram analysis of the spectral image at wavelength (600 nm and 700 nm).

Table A2 The descriptive analysis of the average signals of the different investigated ten *ex vivo* breast samples to highlight the optimum wavelength to differentiate between the normal tissue and the tumor regions.

Wavelength	400	440	480	520	560	600	640
Mean	2.6	20.2	80.1	163.5	211.3	235.8	220.5
Standard Error	0.4	2.3	3.6	18.7	23.9	7.6	24.4
Median	2.6	20.2	80.1	163.5	211.3	235.8	220.5
Standard Deviation ($Ş_d$)	0.5	3.2	5.1	26.4	33.8	10.7	34.5
Sample Variance	0.3	10.5	25.8	699.6	1139.4	115.0	1191.7
Range	0.7	4.6	7.2	37.4	47.7	15.2	48.8
Minimum	2.2	17.9	76.6	144.8	187.4	228.2	196.1
Maximum	3.0	22.5	83.7	182.2	235.1	243.3	244.9
Sum	5.2	40.4	160.3	327.0	422.6	471.5	440.9

Wavelength	680	720	760	800	840	880	920
Mean	185.4	99.4	115.4	50.8	40.2	51.5	21.1
Standard Error	59.6	22.7	47.2	20.1	17.5	21.9	8.6
Median	185.4	99.4	115.4	50.8	40.2	51.5	21.1
Standard Deviation ($Ş_d$)	84.3	32.1	66.8	28.4	24.8	31.0	12.2
Sample Variance	7101.5	1027.2	4459.2	807.9	615.2	963.1	147.7
Range	119.2	45.3	94.4	40.2	35.1	43.9	17.2
Minimum	125.8	76.7	68.2	30.7	22.7	29.6	12.5
Maximum	245.0	122.0	162.6	70.9	57.8	73.5	29.7
Sum	370.8	198.8	230.8	101.5	80.5	103.1	42.2

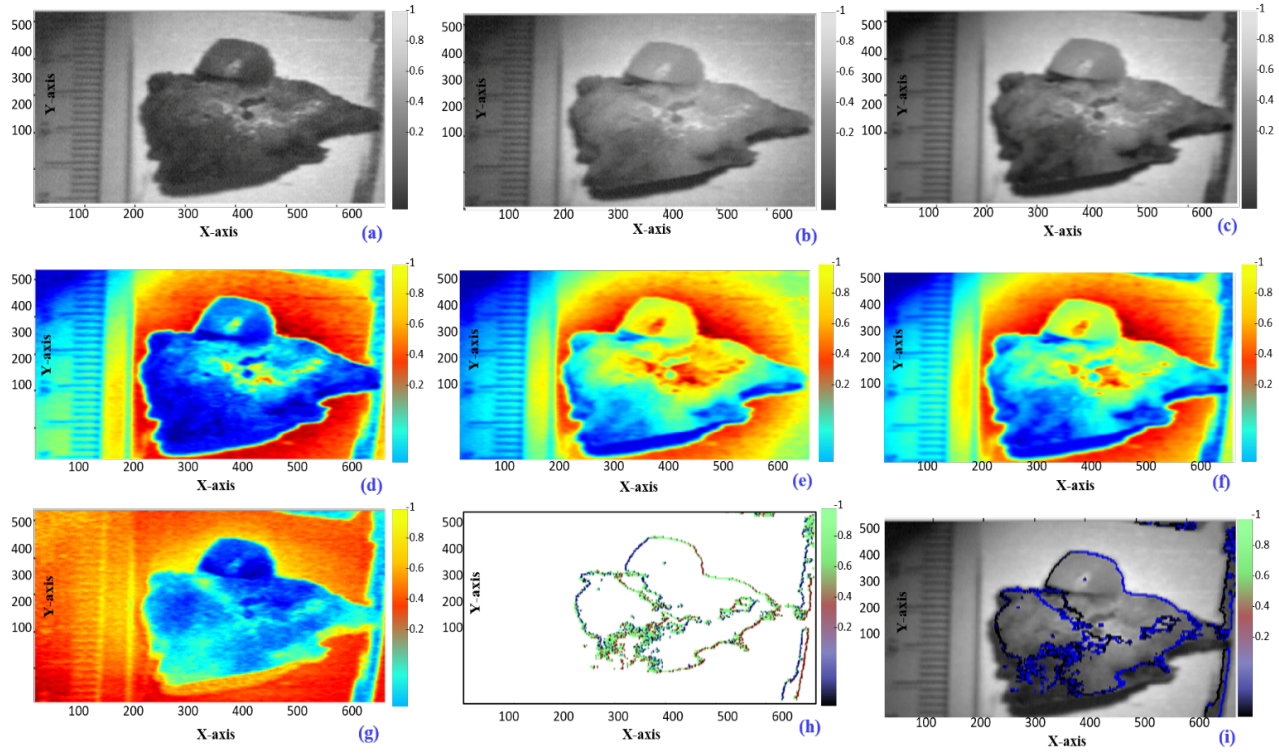

Fig. A6 The worksheet of the investigated *ex vivo* breast Sample #2 to demonstrate the reliability of the applied custom subtraction algorithm to differentiate between the normal tissue and the tumor regions, (a) the *ex vivo* breast sample at wavelength 400 nm, (b) the *ex vivo* breast sample at wavelength 600 nm, (c) the *ex vivo* breast sample at wavelength 700 nm, (d) image enhancement and noise reduction to the scanned to the investigated sample at wavelength 400 nm, (e) image enhancement and noise reduction to the scanned to the investigated sample at wavelength 600 nm, (f) image enhancement and noise reduction to the scanned to the investigated sample at wavelength 700 nm, (g) the subtraction algorithm between the lowest contrast image 400 nm and the highest contrast image 600 nm, (h) the K-mean clustering and the contour mapping of the investigated image, (i) the delineation of the tumor regions applied on the *ex vivo* breast Sample #2.

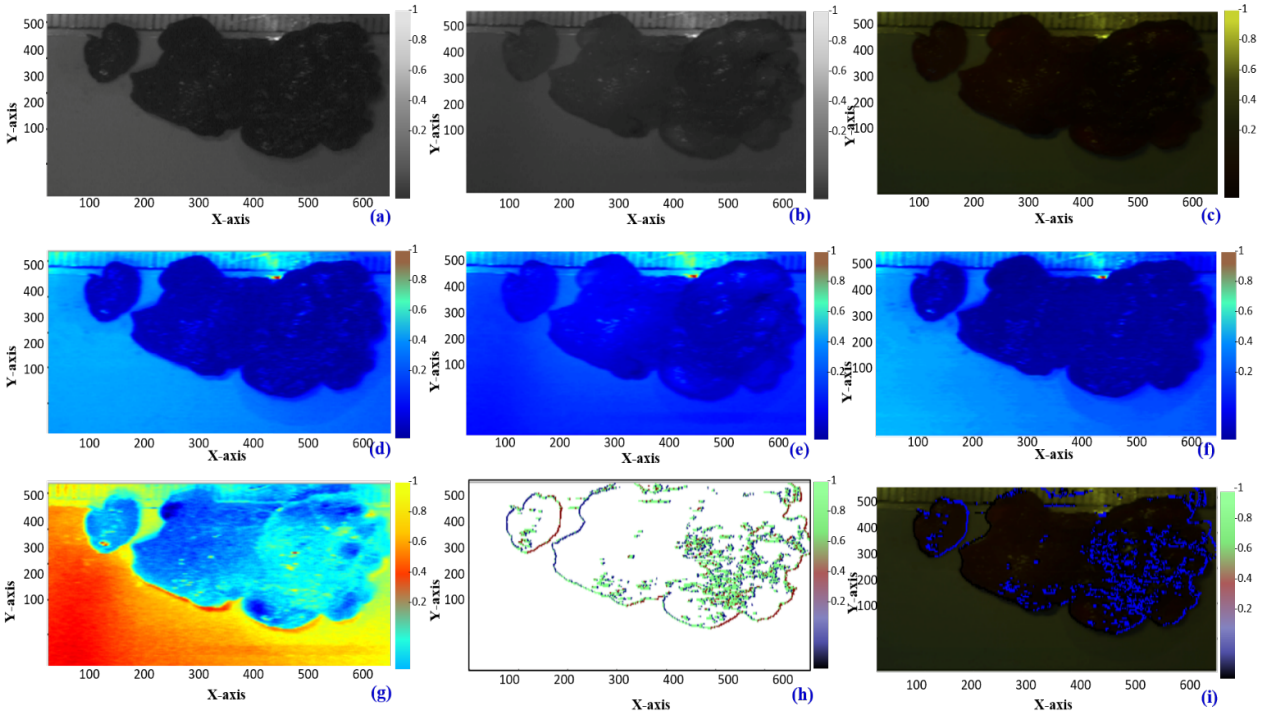

Fig. A7 The worksheet of the investigated *ex vivo* breast sample #3 to demonstrate the reliability of the applied custom subtraction algorithm to differentiate between the normal tissue and the tumor regions, (a) the *ex vivo* breast sample at wavelength 400 nm, (b) the *ex vivo* breast sample at wavelength 600 nm, (c) the *ex vivo* breast sample at wavelength 700 nm, (d) image enhancement and noise reduction to the scanned to the investigated sample at wavelength 400 nm, (e) image enhancement and noise reduction to the scanned to the investigated sample at wavelength 600 nm, (f) image enhancement and noise reduction to the scanned to the investigated sample at wavelength 700 nm, (g) the subtraction algorithm between the lowest contrast image 400 nm and the highest contrast image 600 nm, (h) the K-mean clustering and the contour mapping of the investigated image, (i) the delineation of the tumor regions applied on the *ex vivo* breast Sample #3.

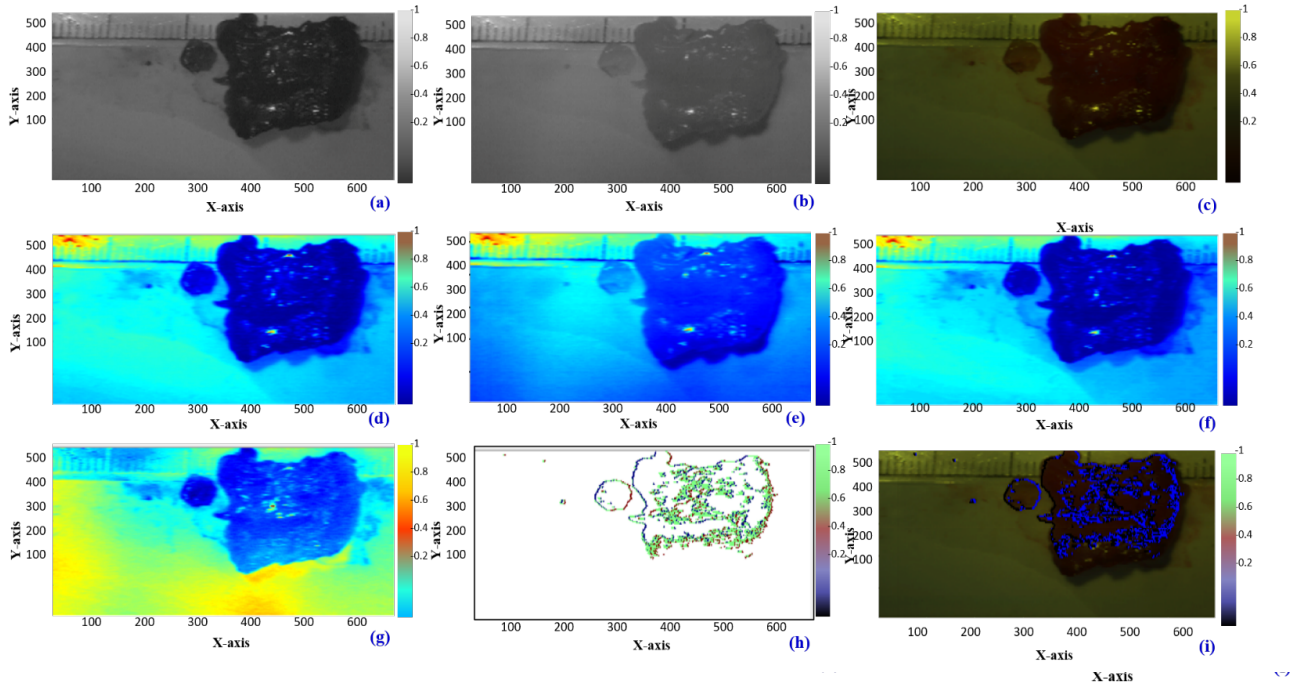

Fig. A8 The worksheet of the investigated *ex vivo* breast Sample #4 to demonstrate the reliability of the applied custom subtraction algorithm to differentiate between the normal tissue and the tumor regions, (a) the *ex vivo* breast sample at wavelength 400 nm, (b) the *ex vivo* breast sample at wavelength 600 nm, (c) the *ex vivo* breast sample at wavelength 700 nm, (d) image enhancement and noise reduction to the scanned to the investigated sample at wavelength 400 nm, (e) image enhancement and noise reduction to the scanned to the investigated sample at wavelength 600 nm, (f) image enhancement and noise reduction to the scanned to the investigated sample at wavelength 700 nm, (g) the subtraction algorithm between the lowest contrast image 400 nm and the highest contrast image 600 nm, (h) the k-mean clustering and the contour mapping of the investigated image, (i) the delineation of the tumor regions applied on the *ex vivo* breast Sample #4.

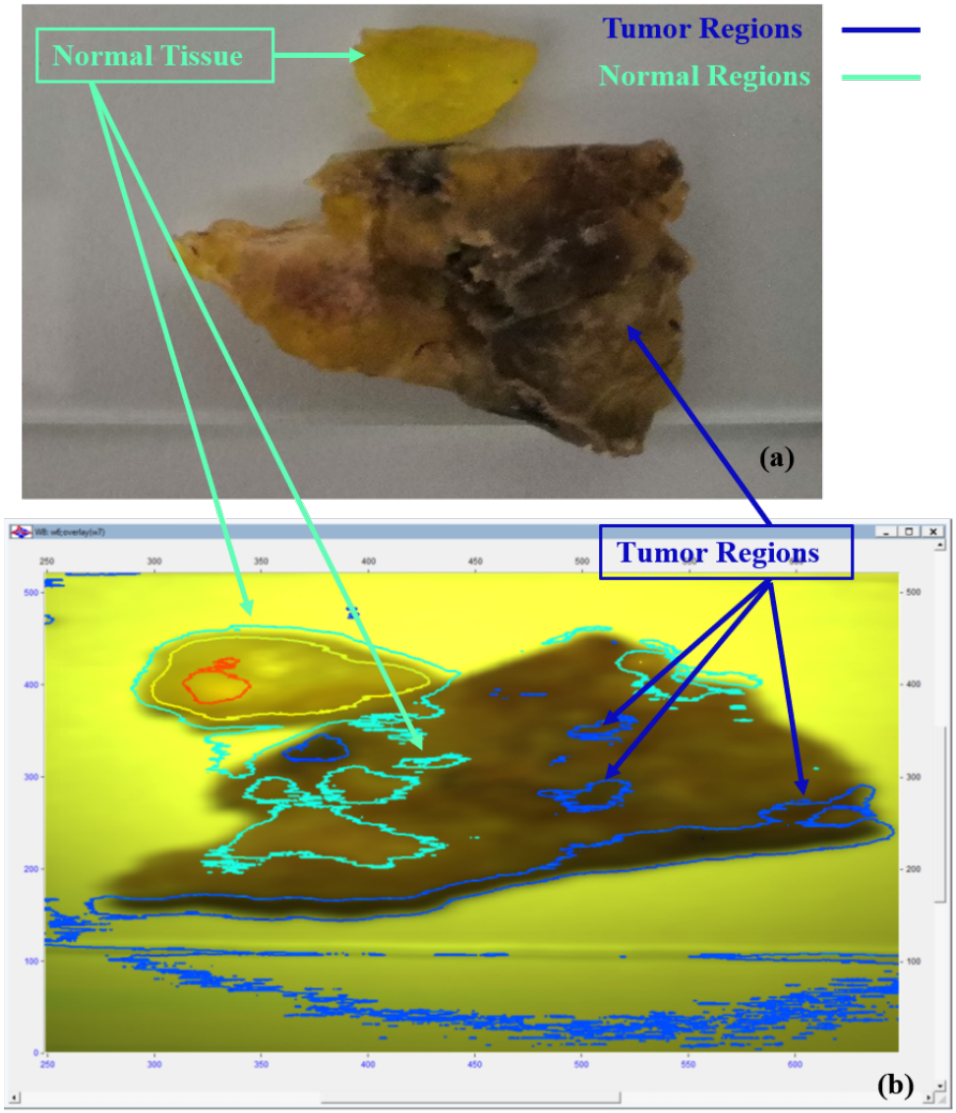

Fig. A9 (a) The investigated RGB image of the *ex vivo* breast Sample #1, (b) the hyperspectral scan image regions after applying the custom algorithm to highlight and contour mapping the normal regions and the various tumor regions.

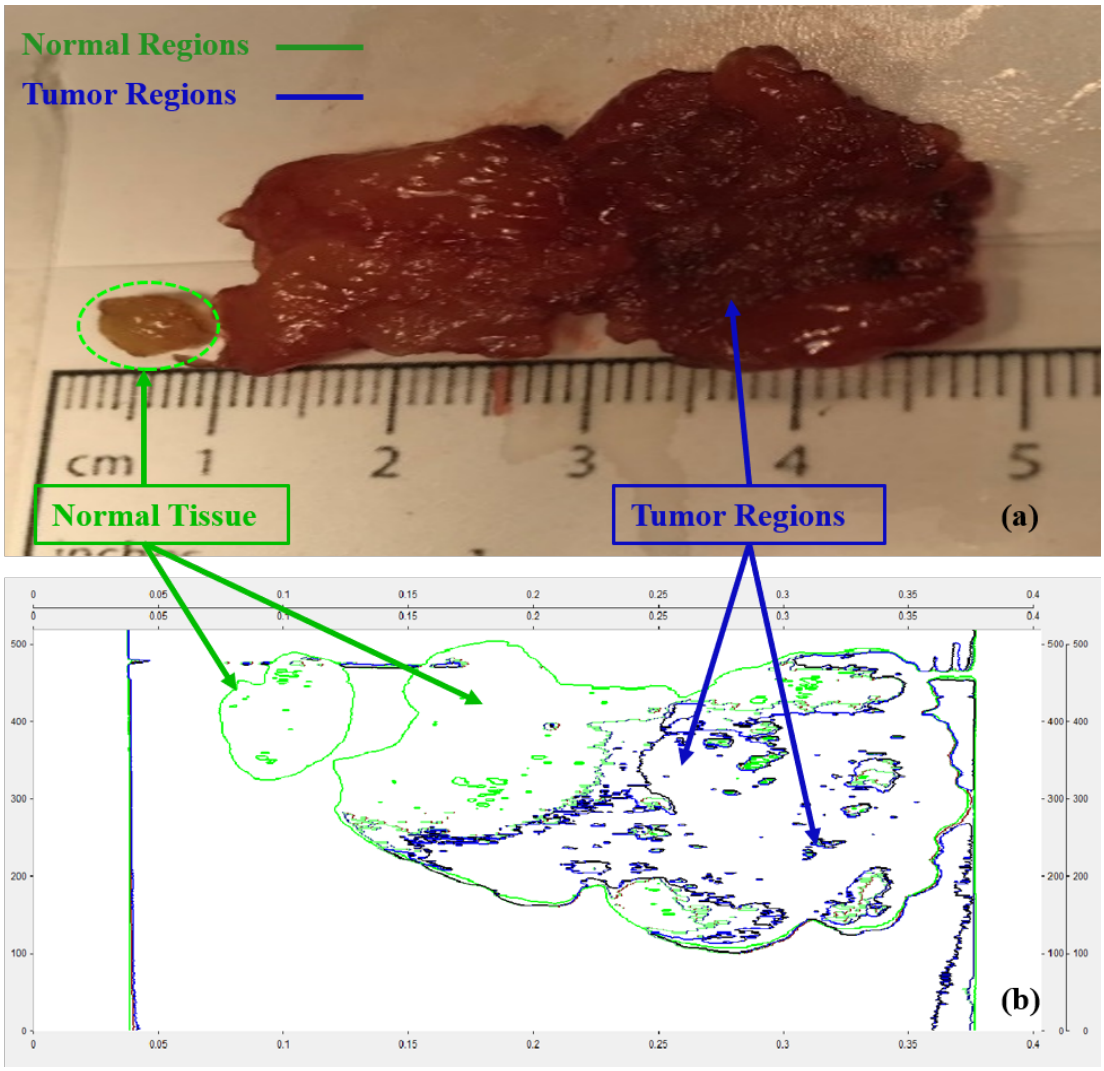

Fig. A10 (a) The investigated RGB image of the *ex vivo* breast Sample #3, (b) the contour mapping of the hyperspectral scan image after applying the custom algorithm to highlight the normal regions and the various tumor regions.